Presented at the ASME Winter Annual Meeting, New Orleans, Louisiana.

ASSESSMENT OF ENERGY-MOMENTUM AND SYMPLECTIC SCHEMES FOR STIFF DYNAMICAL SYSTEMS

J.C. SIMO & O. GONZALEZ

Division of Applied Mechanics
Department of Mechanical Engineering
Stanford University

ABSTRACT

It is shown that conventional symplectic algorithms do not, in general, retain their symplectic character when the symplectic two–form is non–constant. More importantly, it is shown that implicit symplectic schemes are not suitable for the numerical integration of stiff systems possessing high frequency contents. The presence of multiple roots on the unit circle at infinite sampling frequencies leads, inevitably, to eventual blow-up of the scheme if the high frequencies are not resolved. In sharp contrast with symplectic integrators, algorithms designed to simultaneously preserve the total momentum and the energy of the system are shown to be free from these shortcomings. Specifically, for stiff systems, the unresolved high-frequencies are shown to be controlled by property of exact energy conservation without resorting to high-frequency numerical dissipation. A general technique for the construction of exact energy–momentum algorithms is described within the context of the N-body problem.

1. INTRODUCTION AND MOTIVATION.

In recent years, algorithms for Hamiltonian systems that preserve exactly the symplectic character of the Hamiltonian flow have attracted considerable attention in the numerical analysis and geometric mechanics literature; see e.g., the articles of Scovel [1991] and Sanz Serna [1992] for a fairly up to date review of this exponentially growing subject. First introduced in the pioneering work of DeVogelare [1956], symplectic methods are geometrically appealing, but their significance from the standpoint of improved numerical performance remains unsettled. Sharp phase portraits obtained in long numerical simulations are often presented as numerical evidence of improved performance, see e.g., Chanell & Scovel [1990]. However, from the standpoint of (energy) stability in the nonlinear regime, we show by numerical example that symplectic methods can produce disappointing results.

While symplectic algorithms have received much attention in the literature, most of the existing numerical analysis results are implicitly restricted to the case in which the phase space has a symplectic structure induced by a *constant* symplectic matrix. This is the case, for example, when the phase space is either linear or a general

manifold parametrized by local *canonical* coordinates. As will be shown below, the symplectic matrix for a Hamiltonian system need not be constant. For instance, this can occur when the phase space is a general manifold and non-canonical coordinates are used. Given a Hamiltonian system with a nonconstant symplectic matrix, what can we say about conventional 'symplectic' integrators?

The objectives of this contribution are to provide an assessment of the actual performance exhibited by symplectic integrators for simple Hamiltonian systems and to examine the significance of the symplectic condition when the phase space has a symplectic structure induced by a nonconstant symplectic matrix i.e., when the phase space is no longer linear. More specifically, consider a class of algorithms known to be symplectic for Hamiltonian systems on linear spaces. Concrete examples are provided by any of the symplectic members within the class of implicit Runge-Kutta methods, characterized by the condition $\boldsymbol{M} = \boldsymbol{0}$ derived in Lasagni [1988] and Sanz-Serna [1988]. (Here $\boldsymbol{M}$ is the matrix defined in terms of of Butcher's Tableau notation as $\boldsymbol{M} = \boldsymbol{B}\boldsymbol{A} + \boldsymbol{A}^T\boldsymbol{B} - \boldsymbol{b}\boldsymbol{b}^T$; see e.g., Hairer & Wanner [1991] for an explanation of this terminology). The implicit mid-point rule is the classical example whose symplectic character was first noted in Feng Kan [1986]. Concerning these algorithms we ask the following three questions:

a. Do symplectic algorithms retain the symplectic property within the more general context of Hamiltonian systems on manifolds with non-constant symplectic two–form?

b. Do symplectic integrators preserve the Hamiltonian? More importantly, do unconditionally (algebraically) stable symplectic Runge-Kutta methods remain stable regardless of the step-size?

c. Are implicit symplectic integrators suitable for the simulation of stiff systems? (i.e., systems of ODE's possessing a wide spectrum of frequency contents).

Surprisingly, the answer to these three questions is in general *negative*. For instance, for a simple model problem the mid-point rule *fails* to be symplectic when the dynamics are formulated with a nonconstant symplectic matrix. Moreover, symplectic schemes cannot in general conserve the Hamiltonian, unless the system is completely integrable (Ge & Marsden [1989]). Finally, even though the mid–point rule is an algebraically stable Runge-Kutta method, we show algorithms of this type will in general exhibit a severe blow–up for stiff systems. Similar numerical results are observed for symplectic algorithms applied to Galerkin discretizations of infinite-dimensional, non-integrable, Hamiltonian systems (Simo & Tarnow [1992a,b,c]).

An alternative to symplectic integrators are the exact energy-momentum conserving algorithms which, by design, preserve the constants of motion. Specific examples are the technique of Bayliss & Isaacson [1975], the schemes of LaBudde & Greenspan [1976a,b], the integrators for the rotation group of Austin et al [1992] and Simo & Wong [1991], and the energy-momentum method for infinite dimensional

systems of Simo & Tarnow [1992a,b]. Concerning this class of methods we ask the following questions:

d. Is it always possible to construct exact energy-momentum conserving algorithms regardless of the integrability of the Hamiltonian system?

e. Does this task become trivial when working on optimal charts designed to minimize issues such as enforcement of constraints?

f. Does preservation of the Hamiltonian result in enhanced numerical stability?

The answer to the first question is affirmative in general with the construction first proposed in Simo & Tarnow [1992a,b] for infinite dimensional systems and the approach described below being specific examples. Constructions of this type are totally unrelated to any issues pertaining to the integrability of the system. The answer to the second question is, in general, negative. For instance, if we consider the spherical pendulum under constant gravitational loading, the mid-point rule is not symplectic on the unreduced phase space, but conserves energy and momentum since energy and momentum are quadratic constraints on this space. By contrast, in the reduced setting the mid-point rule is symplectic, but no longer preserves energy since the energy constraint ceases to be quadratic. Finally, the answer to the third question is also affirmative. In the simulations of Simo & Tarnow [1992a,b], as well as in the ones described herein, energy-momentum methods are shown to be stable for time steps at which symplectic schemes known to be unconditionally stable in the linear regime experience a dramatic blow-up.

The preceding observations suggest that even for *completely integrable* systems, exemplified by the classical problems considered below, the construction of algorithms that simultaneously preserve the constants of motion as well as the symplectic character of the flow is far from trivial.

2. DYNAMICS OF THE SPHERICAL PENDULUM.

To motivate our subsequent developments consider the simplest, possibly the oldest, model of a nonlinear Hamiltonian dynamical system: the spherical pendulum. Two reasons for this choice are

i. The system is completely integrable for the case of a force field with constant direction, a situation considered below. This allows a direct comparison between the algorithmic flow and the exact flow.

ii. The configuration space is truly a differentiable manifold: the unit sphere. This brings into the problem significant features not present in Hamiltonian systems on linear spaces.

This classical problem provides, therefore, a tractable framework within which the questions raised above can be addressed *explicitly*. If key features fail in a setting

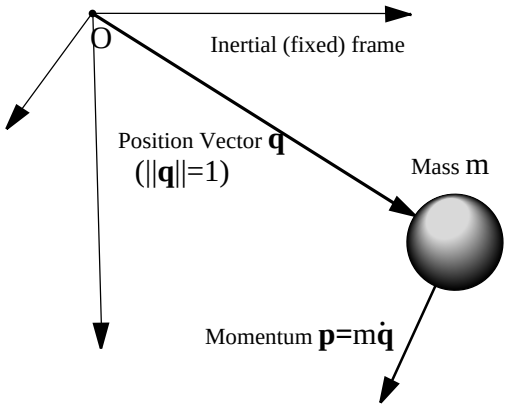

FIGURE 1. The motion of a (spherical) pendulum in the ordinary Euclidean space under a force field.

as simple as the one provided by this model problem, it is unlikely that matters will improve in more complicated situations arising in large-scale simulations.

2.1. Configuration Manifold and Phase Space.

The mechanical system of interest consists of a rigid link of unit length $L = 1$, with one end fixed and the other end attached to a point mass $m > 0$. We choose the fixed end O as the origin of an inertial frame identified with the standard basis in $\mathbb{R}^3$. The possible configurations of the system are thus defined by the vector $\boldsymbol{q}$, directed from the origin O to the mass m, and subject to the constraint $\|\boldsymbol{q}\| = 1$. The configuration space Q for this mechanical system is, therefore, the manifold

$$Q := \{\boldsymbol{q} \in \mathbb{R}^3 : \ h(\boldsymbol{q}) := [\|\boldsymbol{q}\| - 1] = 0\}, \tag{1}$$

which can be identified with the *unit sphere* $S^2 \subset \mathbb{R}^3$. Observe that $\dim[Q] = 2$. Consider a motion of the system $t \mapsto \boldsymbol{q}(t) \in Q$, with velocity $\dot{\boldsymbol{q}}(t)$ and momenta defined via the Legendre transformation $\boldsymbol{p}(t) := m\,\dot{\boldsymbol{q}}(t)$. The constraint $h(\boldsymbol{q}) = 0$ implies that $\boldsymbol{p}$ is also constrained by the condition $\boldsymbol{p} \cdot \boldsymbol{q} = 0$, since

$$\boldsymbol{p} \cdot \boldsymbol{q} = m\dot{\boldsymbol{q}} \cdot \boldsymbol{q} = \tfrac{1}{2} m \frac{d}{dt}\|\boldsymbol{q}\|^2 = 0. \tag{2}$$

One way to satisfy the above constraints is to parametrize the configuration manifold S^2 by a collection of local coordinate patches $\boldsymbol{\chi}: D \to S^2$ from open sets D of $\mathbb{R}^2$ into $S^2 \subset \mathbb{R}^3$ and then formulate the dynamics in terms of the generalized configuration coordinates in D and their conjugate momenta. If the local coordinates on P are canonical, then Hamilton's equations take their familiar canonical form.

While the use of generalized configuration coordinates results in exact enforcement of the constraints, the use of canonical variables can be troublesome. For this

reason it may be more convenient to use non-canonical coordinates on P. Since the configuration space is embedded in $\mathbb{R}^3$, we consider using the natural coordinates of $\mathbb{R}^3$ as coordinates on Q. In this case, the coordinates q^A and their conjugate momenta p_A $(A = 1, 2, 3)$ are not independent and must satisfy the constraints in (1) and (2). The task now is how to *build* these constraints into the dynamics. That is, how can we formulate the dynamics such that the constraints are satisfied. To this end, consider the following alternative choice for the generalized momenta. Let $\boldsymbol{\omega}$ denote the angular velocity of the pendulum in the inertial frame. Then

$$\dot{\boldsymbol{q}} = \boldsymbol{\omega} \times \boldsymbol{q} \tag{3}$$

and, since rotations about the pendulum axis do not enter the dynamics, we have $\boldsymbol{\omega}$ constrained by the relation $\boldsymbol{\omega} \cdot \boldsymbol{q} = 0$. By definition, the angular momentum of the point mass about the origin is $\boldsymbol{\pi} := \boldsymbol{q} \times \boldsymbol{p}$. Using (3), along with the triple cross product identity and the constraint $\boldsymbol{\omega} \cdot \boldsymbol{q} = 0$, we conclude that

$$\boldsymbol{\pi} := \boldsymbol{q} \times \boldsymbol{p} = I_0 \, \boldsymbol{\omega} \quad \text{with} \quad I_0 := mL^2 \quad (L = 1). \tag{4}$$

Taking $\boldsymbol{\pi}$ as the generalized momenta the phase space P for the system can be identified with the set

$$P := \{\boldsymbol{z} = (\boldsymbol{q}, \boldsymbol{\pi}) : \ \boldsymbol{q} \in Q \text{ and } \boldsymbol{\pi} \cdot \boldsymbol{q} = 0\}. \tag{5}$$

Clearly P is a differentiable manifold with $\dim[P] = 4$, and not a linear space. The equations of motion and a symplectic structure on P are defined below.

2.2. Hamilton's Equations: Symplectic Form on P.

Suppose that the pendulum is placed in a force field with potential $V : Q \to \mathbb{R}$. Using equation (3) along with (4) and the balance of angular momentum we obtain the equations of motion

$$\left.\begin{aligned} \dot{\boldsymbol{q}} &= -\,\boldsymbol{q} \times \boldsymbol{\pi} \,/\, I_0 \\ \dot{\boldsymbol{\pi}} &= -\,\boldsymbol{q} \times \nabla V(\boldsymbol{q}) \end{aligned}\right\} \ \text{in } [0, T]. \tag{6a}$$

This system of first order equations, together with the initial data

$$\boldsymbol{q}|_{t=0} = \boldsymbol{q}_0 \quad \text{and} \quad \boldsymbol{\pi}|_{t=0} = \boldsymbol{\pi}_0, \tag{6b}$$

where $\boldsymbol{z}_0 = (\boldsymbol{q}_0, \boldsymbol{\pi}_0) \in P$, completely define the initial value problem for the motion of the pendulum.

Equations (6a) define a Hamiltonian system on the phase space P as follows. Define the Hamiltonian function $H : P \to \mathbb{R}$ as

$$H(\boldsymbol{z}) := \frac{1}{2I_0} \, \|\boldsymbol{\pi}\|^2 + V(\boldsymbol{q}), \tag{7}$$

and consider a two-form $\Omega : TP \times TP \to \mathbb{R}$ given by the expression

$$\Omega(\delta \boldsymbol{z}_1, \delta \boldsymbol{z}_2) := \delta \boldsymbol{z}_1^T \, \mathbb{J}(\boldsymbol{q}) \, \delta \boldsymbol{z}_2, \quad \mathbb{J}(\boldsymbol{q}) := \begin{bmatrix} \mathbf{0} & -\widehat{\boldsymbol{q}} \\ -\widehat{\boldsymbol{q}} & \mathbf{0} \end{bmatrix}, \tag{8a}$$

where $\widehat{\boldsymbol{q}}$ stands for the skew-symmetric matrix with axial vector $\boldsymbol{q}$. Clearly, $\Omega(\cdot, \cdot)$ is a skew-symmetric bilinear form since $\mathbb{J}^T(\boldsymbol{q}) = -\mathbb{J}(\boldsymbol{q})$. Using the triple-product identity, expression (8a) is equivalent to

$$\Omega(\delta \boldsymbol{z}_1, \delta \boldsymbol{z}_2) := -\boldsymbol{q} \cdot (\delta \boldsymbol{\pi}_2 \times \delta \boldsymbol{q}_1 - \delta \boldsymbol{\pi}_1 \times \delta \boldsymbol{q}_2). \tag{8b}$$

In view of (7) and (8), we conclude by inspection that equations (6a) can be written in Hamiltonian form as

$$\dot{\boldsymbol{z}} = \mathbb{J}(\boldsymbol{q}) \nabla H(\boldsymbol{z}) \quad \text{in } [0, T]. \tag{9}$$

In sharp contrast with the situation found when P is a linear space, we note that for the spherical pendulum the symplectic two-form defined by either (8a) or (8b) is configuration dependent. Here the tangent space $T_z P$ at $\boldsymbol{z} \in P$ is the subspace

$$T_z P := \{\delta \boldsymbol{z} = (\delta \boldsymbol{q}, \delta \boldsymbol{\pi}) : \delta \boldsymbol{q} \cdot \boldsymbol{q} = 0 \text{ and } \delta \boldsymbol{\pi} \cdot \boldsymbol{q} = 0\}, \tag{10}$$

which is obtained by enforcing on the admissible variations the linearized version of the constraints on P as defined by (5).

By taking the dot product of $(6a)_{1,2}$ with $\boldsymbol{q}$ one immediately concludes that the flow generated by these equations automatically satisfies the constraint $\|\boldsymbol{q}\| = 1$ together with $\boldsymbol{\pi} \cdot \boldsymbol{q} = 0$, and hence lies in P.

Let $\boldsymbol{F} : P \times [0, T] \to P$ denote the flow generated by (9), assumed to be globally defined for simplicity. Hence, for any $\boldsymbol{z}_0 \in P$ the curve $[0, T] \ni t \mapsto \boldsymbol{z}(t) = \boldsymbol{F}(\boldsymbol{z}_0; t) \in P$ is a solution of (9) with initial condition $\boldsymbol{z}_0$. To verify the symplectic character of $\boldsymbol{F}_t : P \to P$ we proceed as follows. Let $\delta \boldsymbol{z}_\alpha(t)$ $(\alpha = 1, 2)$ denote two arbitrary elements of $T_{z_t} P$ which evolve under the tangent map $D\boldsymbol{F}_t(\boldsymbol{z}_0) : T_{z_0} P \to T_{z_t} P$ i.e., $\delta \boldsymbol{z}_\alpha(t) = D\boldsymbol{F}_t(\boldsymbol{z}_0) \delta \boldsymbol{z}_{0\alpha}$ for some fixed, but arbitrary tangent vectors $\delta \boldsymbol{z}_{0\alpha}$. That the two-form $\Omega : TP \times TP \to \mathbb{R}$ is conserved along the flow can be seen by considering the evolution of $\Omega(t) = \delta \boldsymbol{z}_1(t)^T \mathbb{J}(\boldsymbol{q}(t)) \delta \boldsymbol{z}_2(t)$ as follows. Taking the time derivative of $\Omega(t)$ along the flow gives

$$\dot{\Omega}(t) = \delta \boldsymbol{z}_1^T \mathbb{J}(\dot{\boldsymbol{q}}) \delta \boldsymbol{z}_2 + \delta \dot{\boldsymbol{z}}_1^T \mathbb{J}(\boldsymbol{q}) \delta \boldsymbol{z}_2 + \delta \boldsymbol{z}_1^T \mathbb{J}(\boldsymbol{q}) \delta \dot{\boldsymbol{z}}_2 \tag{11}$$

Consider the first term in (11). A simple calculation using the fact that $\delta \boldsymbol{z}_2 \in T_z P$ shows that $\mathbb{J}(\dot{\boldsymbol{q}}) \delta \boldsymbol{z}_2$ lies in $\mathrm{Ker}[\mathbb{J}(\boldsymbol{q})]$ i.e., $\mathbb{J}(\boldsymbol{q})[\mathbb{J}(\dot{\boldsymbol{q}}) \delta \boldsymbol{z}_2] = \mathbf{0}$. Observing that $T_z P^\perp = \mathrm{Ker}[\mathbb{J}(\boldsymbol{q})]$ we conclude that the first term vanishes since $\delta \boldsymbol{z}_1 \in T_z P$. Using (9) the evolution of the tangent vectors is given by

$$\delta \dot{\boldsymbol{z}}_\alpha = \mathbb{J}(\delta \boldsymbol{q}_\alpha) \nabla H(\boldsymbol{z}) + \mathbb{J}(\boldsymbol{q}) \nabla^2 H(\boldsymbol{z}) \delta \boldsymbol{z}_\alpha \quad (\alpha = 1, 2) \tag{12}$$

Substituting (12) into the last two terms in (11) gives after some straight forward manipulation

$$\dot{\Omega}(t) = 0. \tag{13}$$

The above result, along with the fact that $\Omega(\cdot, \cdot)$ is non-degenerate on TP, verifies that the flow generated by (9) is a symplectic map on P for each $t > 0$.

Remarks. 2.1.

1. One can view $\boldsymbol{q} = (q^1, q^2, q^3)$ as providing a global chart for the unit sphere S^2 much in the same way as the group of unit quaternions provides a global chart for the rotation group $SO(3)$.

2. It is convenient to regard equations (9) as generating a Hamiltonian flow in $\mathbb{R}^3 \times \mathbb{R}^3$, which is constrained by the conditions $\|\boldsymbol{q}\| = 1$ and $\boldsymbol{\pi} \cdot \boldsymbol{q} = 0$ that project the dynamics onto P. The structure of the symplectic matrix $\mathbb{J}(\boldsymbol{q})$ agrees with this approach. Viewed as a 3×3 real matrix $\mathbb{J}(\boldsymbol{q})$ has the two-dimensional null space $\mathrm{Ker}[\mathbb{J}(\boldsymbol{q})] := \mathrm{span}[(\boldsymbol{q}, \boldsymbol{0}), (\boldsymbol{0}, \boldsymbol{q})]$, whose orthogonal complement is precisely $T_z P$ defined by (10). It follows that $\mathbb{J}(\boldsymbol{q})$ restricted to $T_z P$ has rank four, is invertible and satisfies the orthogonality condition $\mathbb{J}(\boldsymbol{q})[\mathbb{J}(\boldsymbol{q})]^T = \mathbf{1}$ since, for any $\boldsymbol{q} \in S^2$, we have

$$-[\widehat{\boldsymbol{q}}\,\widehat{\boldsymbol{q}}]\boldsymbol{a} = \|\boldsymbol{q}\|^2 \boldsymbol{a} - (\boldsymbol{q} \cdot \boldsymbol{a})\boldsymbol{q} = \boldsymbol{a} \qquad \forall \boldsymbol{a} \in \mathbb{R}^3, \;\; \boldsymbol{a} \cdot \boldsymbol{q} = 0. \tag{14}$$

3. In a gravitational field with constant direction $\boldsymbol{\gamma}$ ($\|\boldsymbol{\gamma}\| = 1$) and variable intensity defined by the function $g : \mathbb{R} \to \mathbb{R}$, the potential energy and the equation of motion $(6\mathrm{a})_2$ reduce to

$$V(\boldsymbol{q}) = -g(\boldsymbol{\gamma} \cdot \boldsymbol{q}) \quad \text{and} \quad \dot{\boldsymbol{\pi}} = g'(\boldsymbol{\gamma} \cdot \boldsymbol{q})\, \boldsymbol{q} \times \boldsymbol{\gamma}, \tag{15}$$

respectively. The invariance of the Hamiltonian under the circle group S^1 of rotations about $\boldsymbol{\gamma}$ yields the additional conserved quantity

$$J_\gamma := \boldsymbol{\pi} \cdot \boldsymbol{\gamma} \quad \text{since} \quad \dot{J}_\gamma = \dot{\boldsymbol{\pi}} \cdot \boldsymbol{\gamma} = 0, \tag{16}$$

as a result of (15). The momentum map $J_\gamma : P \to \mathbb{R}$ gives the angular momentum about the gravity axis. □

Before proceeding with the analysis of algorithmic approximations on P we first introduce the notion of symplectic reduction which will be used in the following sections to illustrate a number of algorithmic issues.

2.3. The Case of a Gravitational Field: Reduction.

Consider the dynamics of the pendulum in a gravitational field. Due to the presence of the conserved quantity J_γ the dynamics may be formulated on a reduced phase space $\tilde{P}$ as follows. Assume for simplicity that the initial position $\boldsymbol{q}_0$, the initial momentum $\boldsymbol{p}_0$ normal to $\boldsymbol{q}_0$, and the gravity axis $\boldsymbol{\gamma}$ all lie in a plane with unit normal $\boldsymbol{e}_2$. It then follows that

$$\boldsymbol{\pi}_0 = \boldsymbol{q}_0 \times \boldsymbol{p}_0 = \pi_0 \boldsymbol{e}_2 \quad \text{and} \quad J_\gamma = \boldsymbol{\gamma} \cdot \boldsymbol{\pi}_0 = 0, \tag{17}$$

where $\pi_0 = \|\boldsymbol{p}_0\|$. The presence of two conserved quantities, the Hamiltonian H and the angular momentum J_γ about the gravitational axis, yields a reduced phase space

$\widetilde{P}$ of dimension $\dim[\widetilde{P}] = 4 - 2 = 2$. Hence, the reduced dynamics is completely integrable and takes place on the level set $J_\gamma^{-1}(0) \subset P$ of zero angular momentum modulo rotations about $\boldsymbol{\gamma}$, i.e.,

$$\widetilde{Q} = Q/S^1 \approx S^1 \quad \text{and} \quad \tilde{P} = J_\gamma^{-1}(0)/S^1 \approx \mathbb{T}^2. \tag{18}$$

The reduced configuration space is therefore the unit circle S^1 (identified with the real line modulo 2π angles), while the reduced phase space can be identified with the torus $\mathbb{T}^2$.

The reduced dynamics takes place in the plane normal to $\boldsymbol{e}_2$ and is governed by the following classical equations. Consider the basis $\{\boldsymbol{e}_1, \boldsymbol{e}_2, \boldsymbol{e}_3\}$ with $\boldsymbol{e}_3 = \boldsymbol{\gamma}$ and $\boldsymbol{e}_1 := \boldsymbol{e}_2 \times \boldsymbol{e}_3$, and let ϑ denote the angle between $\boldsymbol{q}$ and $\boldsymbol{e}_3$ so that

$$\boldsymbol{q} = [\cos(\vartheta)\boldsymbol{e}_3 + \sin(\vartheta)\boldsymbol{e}_1] \quad \text{and} \quad \boldsymbol{\pi} = I_0\, \dot{\vartheta}\, \boldsymbol{e}_2. \tag{19}$$

Using $(19)_1$ we have that $\boldsymbol{q} \times \nabla V(\boldsymbol{q}) = g'(\cos(\vartheta))\sin(\vartheta)\boldsymbol{e}_2$ and Hamilton's equations (6) collapse to the system

$$\left.\begin{aligned} \dot{\vartheta} &= \pi \,/\, I_0 \\ \dot{\pi} &= -g'(\cos(\vartheta))\sin(\vartheta) \end{aligned}\right\} \text{ in } [0,T], \tag{20a}$$

subject to the initial conditions

$$\vartheta|_{t=0} = \vartheta_0 \quad \text{and} \quad \pi|_{t=0} = \pi_0. \tag{20b}$$

Setting $\tilde{\boldsymbol{z}} = (\vartheta, \pi) \in \tilde{P}$, equations (20a) are Hamiltonian with reduced Hamiltonian function $\widetilde{H} : \tilde{P} \to \mathbb{R}$ given by

$$\tilde{H}(\tilde{\boldsymbol{z}}) := \frac{1}{2I_0}\,\pi^2 - g(\cos(\vartheta)), \tag{21}$$

relative to the canonical symplectic two-form on $\mathbb{R}^2$

$$\widetilde{\Omega}(\delta\tilde{\boldsymbol{z}}_1, \delta\tilde{\boldsymbol{z}}_2) := \delta\tilde{\boldsymbol{z}}_1 \cdot \widetilde{\mathbb{J}}\delta\tilde{\boldsymbol{z}}_2 \quad \text{where} \quad \widetilde{\mathbb{J}} := \begin{bmatrix} 0 & 1 \\ -1 & 0 \end{bmatrix}. \tag{22}$$

In fact, inspection of (20a) reveals that this system can be written as

$$\dot{\tilde{\boldsymbol{z}}} = \widetilde{\mathbb{J}}\nabla\widetilde{H}(\tilde{\boldsymbol{z}}) \quad \text{in } [0,T], \tag{23}$$

in agreement with the abstract symplectic reduction theorem (see Abraham & Marsden [1978, page 347]). A result exploited in the analysis below is that *the reduced dynamics is Hamiltonian relative to* (22) *if and only if the original dynamics is Hamiltonian relative to* (8). That the reduced symplectic structure (22) happens to be canonical is a specific feature of this elementary example (the symmetry group of rotations about γ is abelian) which does not carry over to the general case.

3. ALGORITHMIC APPROXIMATIONS ON P.

The analysis below is aimed at illustrating the following points raised in the introduction. First, algorithms known to be symplectic on linear spaces need not retain this property on general manifolds. Second, symplectic algorithms need not, and in general will not, conserve energy. We will illustrate these points by considering a conventional mid-point approximation to the Hamiltonian flow generated by (9) and showing that this scheme, well-known to be symplectic on linear spaces, no longer retains the symplectic property for the problem at hand.

That 'optimal' charts do not necessarily render trivial the conservation of the constants of motion will be illustrated below by reformulating the mid-point rule directly on the reduced space $\widetilde{P}$, with canonical symplectic structure defined by (22). In this setting, this algorithm retains its symplectic character but the property of exact energy conservation is lost since the Hamiltonian is no longer quadratic. Conventional higher order symplectic Runge-Kutta methods will not improve on this situation, the underlying reason being that the function $\cos(\cdot)$ cannot be integrated exactly regardless of the order of accuracy of the method.

Finally, we describe a symplectic scheme on the reduced phase space which when lifted to the unreduced phase space by a reconstruction procedure yields a symplectic scheme on P. This scheme, however, does not fall within the class of conventional Runge-Kutta methods.

3.1. Mid-point Approximation on P.

Let $[0,T] = \cup_{n=0}^{N}[t_n, t_{n+1}]$ be a partition of the time interval of interest. Suppose one is given initial data $\boldsymbol{z}_n = (\boldsymbol{q}_n, \boldsymbol{\pi}_n) \in P$ at time t_n, where $\boldsymbol{z}_n$ stands for an algorithmic approximation to $\boldsymbol{z}(t_n)$, and consider the mid-point approximation

$$\boldsymbol{z}_{n+1} - \boldsymbol{z}_n = \Delta t \mathbb{J}(\boldsymbol{q}_{n+\frac{1}{2}}) \nabla H(\boldsymbol{z}_{n+\frac{1}{2}}) \tag{24a}$$

with $\boldsymbol{z}_{n+\frac{1}{2}} := (\boldsymbol{q}_{n+\frac{1}{2}}, \boldsymbol{\pi}_{n+\frac{1}{2}})$, where $\boldsymbol{q}_{n+\frac{1}{2}} := \frac{1}{2}(\boldsymbol{q}_n + \boldsymbol{q}_{n+1})$ and $\boldsymbol{\pi}_{n+\frac{1}{2}} := \frac{1}{2}(\boldsymbol{\pi}_n + \boldsymbol{\pi}_{n+1})$. As mentioned above, this algorithm would be symplectic if P were a linear space (with $\mathbb{J}$ therefore constant). In view of (7) and (8) the explicit form of (24a) is

$$\left.\begin{aligned} \boldsymbol{q}_{n+1} - \boldsymbol{q}_n &= -\Delta t\, \boldsymbol{q}_{n+\frac{1}{2}} \times \boldsymbol{\pi}_{n+\frac{1}{2}}/I_0 \\ \boldsymbol{\pi}_{n+1} - \boldsymbol{\pi}_n &= -\Delta t\, \boldsymbol{q}_{n+\frac{1}{2}} \times \nabla V(\boldsymbol{q}_{n+\frac{1}{2}}) \end{aligned}\right\}. \tag{24b}$$

This approximation possesses the following noteworthy feature.

Lemma 3.1. The algorithmic flow generated by (24) does in fact lie in the phase space P, i.e., $\boldsymbol{z}_n = (\boldsymbol{q}_n, \boldsymbol{\pi}_n) \in P$ for $n = 1, 2, \cdots, N$, if the initial data $\boldsymbol{z}_0 = (\boldsymbol{q}_0, \boldsymbol{\pi}_0)$ is in P.

Proof. Assume that $\boldsymbol{z}_n \in P$. Taking the dot product of $(24\text{b})_1$ with $\boldsymbol{q}_{n+\frac{1}{2}}$ yields

$$\boldsymbol{q}_{n+\frac{1}{2}} \cdot (\boldsymbol{q}_{n+1} - \boldsymbol{q}_n) = \tfrac{1}{2}[\|\boldsymbol{q}_{n+1}\|^2 - \|\boldsymbol{q}_n\|^2] = 0, \tag{25}$$

which implies that $\boldsymbol{q}_{n+1} \in Q$. Now observe that $\boldsymbol{\pi}_{n+\frac{1}{2}} \cdot (\boldsymbol{q}_{n+1} - \boldsymbol{q}_n) = 0$ as a result of $(24\text{b})_1$ and $\boldsymbol{q}_{n+\frac{1}{2}} \cdot (\boldsymbol{\pi}_{n+1} - \boldsymbol{\pi}_n) = 0$ as a result of $(24\text{b})_2$. Making use of the identity

$$\begin{aligned} \boldsymbol{\pi}_{n+1} \cdot \boldsymbol{q}_{n+1} - \boldsymbol{\pi}_n \cdot \boldsymbol{q}_n &= \boldsymbol{q}_{n+\frac{1}{2}} \cdot (\boldsymbol{\pi}_{n+1} - \boldsymbol{\pi}_n) \\ &\quad + \boldsymbol{\pi}_{n+\frac{1}{2}} \cdot (\boldsymbol{q}_{n+1} - \boldsymbol{q}_n) \end{aligned} \tag{26}$$

we conclude that $\boldsymbol{\pi}_{n+1} \cdot \boldsymbol{q}_{n+1} = 0$ since $\boldsymbol{z}_n \in P$. Hence $\boldsymbol{z}_{n+1} \in P$ as claimed. □

By setting $\Delta \boldsymbol{z} := \boldsymbol{z}_{n+1} - \boldsymbol{z}_n$ and $\boldsymbol{z}_{n+\frac{1}{2}} = \boldsymbol{z}_n + \frac{1}{2}\Delta \boldsymbol{z}$ we can view (24a) as a non-linear algebraic system in the unknown $\Delta \boldsymbol{z}$. Observe that $\Delta \boldsymbol{z}$ lies in the orthogonal complement $\ker^{\perp}[\mathbb{J}(\boldsymbol{q}_{n+\frac{1}{2}})]$ to the null space of $\mathbb{J}(\boldsymbol{q}_{n+\frac{1}{2}})$ given by

$$\ker[\mathbb{J}(\boldsymbol{q}_{n+\frac{1}{2}})] = \operatorname{span}\{(\boldsymbol{q}_{n+\frac{1}{2}}, \boldsymbol{0}), (\boldsymbol{0}, \boldsymbol{q}_{n+\frac{1}{2}})\}. \tag{27}$$

The restriction of the matrix $\mathbb{J}(\boldsymbol{q}_{n+\frac{1}{2}})$ to the solution space $\ker^{\perp}[\mathbb{J}(\boldsymbol{q}_{n+\frac{1}{2}})]$ is as discussed above non-singular and skew-symmetric. However, it is no longer *orthogonal.* To see this, consider

$$\mathbb{J}(\boldsymbol{q}_{n+\frac{1}{2}})[\mathbb{J}(\boldsymbol{q}_{n+\frac{1}{2}})]^T = \begin{bmatrix} -\widehat{\boldsymbol{q}}_{n+\frac{1}{2}}\widehat{\boldsymbol{q}}_{n+\frac{1}{2}} & \boldsymbol{0} \\ \boldsymbol{0} & -\widehat{\boldsymbol{q}}_{n+\frac{1}{2}}\widehat{\boldsymbol{q}}_{n+\frac{1}{2}} \end{bmatrix} \tag{28}$$

and note that since $\boldsymbol{q}_{n+\frac{1}{2}} \notin Q$ it follows that $\|\boldsymbol{q}_{n+\frac{1}{2}}\| \neq 1$. Therefore, for any $\boldsymbol{a}$ such that $\boldsymbol{a} \cdot \boldsymbol{q}_{n+\frac{1}{2}} = 0$ we have

$$-[\widehat{\boldsymbol{q}}_{n+\frac{1}{2}}\widehat{\boldsymbol{q}}_{n+\frac{1}{2}}]\boldsymbol{a} = \|\boldsymbol{q}_{n+\frac{1}{2}}\|^2 \boldsymbol{a} \neq \boldsymbol{a}, \tag{29}$$

It is precisely this lack of orthogonality in the mid-point approximation $\mathbb{J}(\boldsymbol{q}_{n+\frac{1}{2}})$ that renders algorithm (24) non-symplectic, A direct verification of this result involves computing the transition matrix $\boldsymbol{A}_{\Delta t}(\boldsymbol{z}_n, \boldsymbol{z}_{n+1})$ of the linearized algorithmic dynamics, i.e.,

$$\delta \boldsymbol{z}_{n+1} = \boldsymbol{A}_{\Delta t}(\boldsymbol{z}_n, \boldsymbol{z}_{n+1})\, \delta \boldsymbol{z}_n, \tag{30}$$

and checking by a brute-force calculation the failure of the symplectic condition

$$[\boldsymbol{A}_{\Delta t}(\boldsymbol{z}_n, \boldsymbol{z}_{n+1})]^T \mathbb{J}(\boldsymbol{q}_{n+1}) \boldsymbol{A}_{\Delta t}(\boldsymbol{z}_n, \boldsymbol{z}_{n+1}) \neq \mathbb{J}(\boldsymbol{q}_n). \tag{31}$$

Remarks. 3.1.

1. Observe that equation $(24b)_1$ can be solved for $\boldsymbol{q}_{n+1}$ explicitly to obtain

$$\boldsymbol{q}_{n+1} = \text{cay}[\Delta t \widehat{\boldsymbol{\pi}}_{n+\frac{1}{2}}/I_0]\, \boldsymbol{q}_n, \tag{32}$$

where $\text{cay} : \mathbb{R}^3 \to SO(3)$ is the Cayley transform given by the expression (see Simo, Tarnow & Doblaré [1992])

$$\text{cay}[\boldsymbol{\vartheta}] = \mathbf{1} + \frac{2}{1 + \frac{1}{4}\|\boldsymbol{\vartheta}\|^2}\left[\tfrac{1}{2}\widehat{\boldsymbol{\vartheta}} + \tfrac{1}{4}\widehat{\boldsymbol{\vartheta}}^2\right]. \tag{33}$$

That $\text{cay}[\boldsymbol{\vartheta}]$ is a proper orthogonal matrix can be verified by a direct computation.

2. In general, algorithm (24) does not conserve energy. Let $K(\boldsymbol{\pi}) := \frac{1}{2}\|\boldsymbol{\pi}\|^2/I_0$ denote the kinetic energy. By taking the dot product of $(24b)_2$ with $\boldsymbol{\pi}_{n+\frac{1}{2}}$ and using $(24b)_1$ we arrive at

$$K(\boldsymbol{\pi}_{n+1}) - K(\boldsymbol{\pi}_n) = -(\boldsymbol{q}_{n+1} - \boldsymbol{q}_n) \cdot \nabla V(\boldsymbol{q}_{n+\frac{1}{2}}). \tag{34}$$

Since $H(\boldsymbol{z}) = K(\boldsymbol{\pi}) + V(\boldsymbol{q})$, the Hamiltonian is exactly conserved if and only if

$$V(\boldsymbol{q}_{n+1}) - V(\boldsymbol{q}_n) = (\boldsymbol{q}_{n+1} - \boldsymbol{q}_n) \cdot \nabla V(\boldsymbol{q}_{n+\frac{1}{2}}); \tag{35}$$

an equality which holds in general only if $V(\boldsymbol{q})$ is a *quadratic form* in $\boldsymbol{q}$.

3. Consider a gravitational field with $\nabla V(\boldsymbol{q}) := -g'(\boldsymbol{q} \cdot \boldsymbol{\gamma})\,\boldsymbol{\gamma}$ ($\boldsymbol{\gamma}$ = constant). From the preceding remark we conclude that energy is generally not preserved unless $g(\cdot)$ is at most quadratic. On the other hand, since

$$J_\gamma(\boldsymbol{z}_{n+1}) - J_\gamma(\boldsymbol{z}_n) = (\boldsymbol{\pi}_{n+1} - \boldsymbol{\pi}_n) \cdot \gamma = 0 \tag{36}$$

algorithm (24) exactly conserves momentum. □

In summary, the preceding analysis shows that the classical mid-point rule *does not retain its symplectic character for the pendulum problem formulated on* P and is not energy-conserving in general. In the next section we verify this result by applying the symplectic reduction theorem. There, however, we consider an even simpler problem: the dynamics of the pendulum in a gravitational field.

3.2. Algorithmic Reduction.

Since (24) is momentum preserving if the potential function is that of a gravitational field, the *discrete* dynamics also drop to the reduced manifold $\widetilde{P} = \mathbb{T}^2$. This reduction can be carried out explicitly as follows.

As in the continuum problem, choose the basis $\{\boldsymbol{e}_1, \boldsymbol{e}_2, \boldsymbol{e}_3\}$ with $\boldsymbol{e}_3 = \boldsymbol{\gamma}$, the initial data $\boldsymbol{q}_0$ in the plane normal to $\boldsymbol{e}_2$, and $\boldsymbol{\pi}_0 = \pi_0 \boldsymbol{e}_2$ directed along $\boldsymbol{e}_2$. From the algorithmic dynamics (24b) one easily concludes that $\boldsymbol{q}_n$, $\boldsymbol{q}_{n+1}$ and $\boldsymbol{q}_{n+\frac{1}{2}}$ remain in the plane normal to $\boldsymbol{e}_2$ and $\boldsymbol{\pi}_n$, $\boldsymbol{\pi}_{n+\frac{1}{2}}$ and $\boldsymbol{\pi}_{n+1}$ are directed along $\boldsymbol{e}_2$. Set

$$\left.\begin{aligned} \boldsymbol{q}_{n+1} &= [\cos(\vartheta_{n+1})\boldsymbol{e}_3 + \sin(\vartheta_{n+1})\boldsymbol{e}_1] \\ \boldsymbol{q}_n &= [\cos(\vartheta_n)\boldsymbol{e}_3 + \sin(\vartheta_n)\boldsymbol{e}_1] \end{aligned}\right\} \tag{37}$$

and let $\vartheta := \vartheta_{n+1} - \vartheta_n$ be the angle between $\boldsymbol{q}_n$ and $\boldsymbol{q}_{n+1}$. Now use elementary trigonometric identities to conclude that

$$\|\boldsymbol{q}_{n+\frac{1}{2}}\|^2 = \tfrac{1}{2}[1 + \cos(\vartheta)] = \cos^2(\tfrac{1}{2}\vartheta). \tag{38}$$

Since $\boldsymbol{q}_n$, $\boldsymbol{q}_{n+\frac{1}{2}}$, and $\boldsymbol{q}_{n+1}$ are in the plane normal to $\boldsymbol{\pi}_n$, $\boldsymbol{\pi}_{n+\frac{1}{2}}$, and $\boldsymbol{\pi}_{n+1}$, equation $(24b)_1$ along with (38) and an elementary trigonometric identity give

$$\boldsymbol{\pi}_{n+\frac{1}{2}} = \frac{I_0}{\Delta t}\,(\boldsymbol{q}_n \times \boldsymbol{q}_{n+1})/\|\boldsymbol{q}_{n+\frac{1}{2}}\|^2 = 2\,\frac{I_0}{\Delta t}\,\tan(\tfrac{1}{2}\vartheta)\,\boldsymbol{e}_2; \tag{39}$$

a relation which can be rewritten as

$$\vartheta_{n+1} - \vartheta_n = \Delta t \kappa_1\, \pi_{n+\frac{1}{2}}/I_0 \quad \text{with} \quad \kappa_1 := \frac{\vartheta/2}{\tan(\frac{1}{2}\vartheta)} \tag{40}$$

The reduction is completed by evaluating the right-hand-side of $(24b)_2$ with the aid of trigonometric identities. Setting $\vartheta_{n+\frac{1}{2}} := \frac{1}{2}(\vartheta_{n+1} + \vartheta_n)$ the reduced equations for the algorithmic flow take the following form

$$\left.\begin{aligned} \vartheta_{n+1} - \vartheta_n &= \quad \Delta t\, \kappa_1\, \pi_{n+\frac{1}{2}}\,/\,I_0 \\ \pi_{n+1} - \pi_n &= -\Delta t\, \kappa_2\, g'(\kappa_2 \cos(\vartheta_{n+\frac{1}{2}}))\sin(\vartheta_{n+\frac{1}{2}}) \end{aligned}\right\} \tag{41}$$

where κ_α $(\alpha = 1, 2)$ are functions of $(\vartheta_n, \vartheta_{n+1})$ defined in the present context as

$$\kappa_1 := \frac{(\vartheta_{n+1} - \vartheta_n)/2}{\tan(\frac{1}{2}(\vartheta_{n+1} - \vartheta_n))}, \quad \kappa_2 := \cos(\tfrac{1}{2}(\vartheta_{n+1} - \vartheta_n)). \tag{42}$$

Observe that κ_1 and κ_2 so defined differ from unity by terms of order Δt^2, i.e., $\kappa_\alpha(\vartheta_n, \vartheta_{n+1}) = 1 + \mathcal{O}(\Delta t^2)$ $(\alpha = 1, 2)$.

The foregoing analysis shows that algorithm (41) restricted by conditions (42) is equivalent to the conventional mid-point rule (24) formulated on the unreduced phase space P. Does this scheme, well-known to define a symplectic transformation if P were linear, retain its symplectic character within the present context? By the symplectic reduction theorem, the mid-point rule (24) formulated on P is symplectic if and only if the reduced algorithm (41) subject to (42) is symplectic on $\tilde{P}$. The following result, derived for arbitrary functions κ_α, shows that this is not the case.

Lemma 3.2. Algorithm (41) with κ_1 and κ_2 viewed as arbitrary functions on $\widetilde{Q} \times \widetilde{Q}$ subject to the consistency requirement $\kappa_\alpha(\vartheta_n, \vartheta_{n+1}) = 1 + \mathcal{O}(\Delta t^2)$ $(\alpha = 1, 2)$ is symplectic if

$$\frac{\partial \kappa_1}{\partial \vartheta_1} + \frac{\partial \kappa_1}{\partial \vartheta_2} = 0 \quad \text{and} \quad \frac{\partial \kappa_2}{\partial \vartheta_1} - \frac{\partial \kappa_2}{\partial \vartheta_2} = 0 \tag{43}$$

where $\vartheta_1 = \vartheta_n$ and $\vartheta_2 = \vartheta_{n+1}$.

Proof. Set $g'_{n+\frac{1}{2}} := g'(\kappa_2 \cos(\vartheta_{n+\frac{1}{2}}))$ and let $\widetilde{\boldsymbol{A}}_{\Delta t}(\tilde{\boldsymbol{z}}_n, \tilde{\boldsymbol{z}}_{n+1})$ denote the transition matrix of the linearized algorithmic dynamics, i.e.,

$$\delta \tilde{\boldsymbol{z}}_{n+1} = \widetilde{\boldsymbol{A}}_{\Delta t}(\tilde{\boldsymbol{z}}_n, \tilde{\boldsymbol{z}}_{n+1})\, \delta \tilde{\boldsymbol{z}}_n. \tag{44}$$

From (41) it follows that $\widetilde{\boldsymbol{A}}_{\Delta t}(\tilde{\boldsymbol{z}}_n, \tilde{\boldsymbol{z}}_{n+1}) = \boldsymbol{B}_1^{-1} \boldsymbol{B}_0$, where

$$\boldsymbol{B}_1 := \begin{bmatrix} 1 - \frac{\Delta t \kappa_{1,2} \pi_{n+\frac{1}{2}}}{I_0} & -\frac{\Delta t \kappa_1}{2 I_0} \\ b_1 & 1 \end{bmatrix}, \tag{45a}$$

and

$$\boldsymbol{B}_0 := \begin{bmatrix} 1 + \frac{\Delta t \kappa_{1,1} \pi_{n+\frac{1}{2}}}{I_0} & \frac{\Delta t \kappa_1}{2 I_0} \\ -b_0 & 1 \end{bmatrix} \tag{46b}$$

with b_0 and b_1 defined by

$$\begin{aligned} b_1 := \Delta t \Big[& g'_{n+\frac{1}{2}} [\tfrac{1}{2} \kappa_2 \cos(\vartheta_{n+\frac{1}{2}}) + \kappa_{2,2} \sin(\vartheta_{n+\frac{1}{2}})] \\ & - g''_{n+\frac{1}{2}} [\tfrac{1}{2} \kappa_2 \sin(\vartheta_{n+\frac{1}{2}}) - \kappa_{2,2} \cos(\vartheta_{n+\frac{1}{2}})] \kappa_2 \sin(\vartheta_{n+\frac{1}{2}}) \Big] \\ b_0 := \Delta t \Big[& g'_{n+\frac{1}{2}} [\tfrac{1}{2} \kappa_2 \cos(\vartheta_{n+\frac{1}{2}}) + \kappa_{2,1} \sin(\vartheta_{n+\frac{1}{2}})] \\ & - g''_{n+\frac{1}{2}} [\tfrac{1}{2} \kappa_2 \sin(\vartheta_{n+\frac{1}{2}}) - \kappa_{2,1} \cos(\vartheta_{n+\frac{1}{2}})] \kappa_2 \sin(\vartheta_{n+\frac{1}{2}}) \Big] \end{aligned}$$

Now recall that for a one degree of freedom system the symplectic condition reduces to the requirement that the transition matrix be volume preserving. Consequently,

$$\det \Big[\widetilde{\boldsymbol{A}}_{\Delta t}(\tilde{\boldsymbol{z}}_n, \tilde{\boldsymbol{z}}_{n+1}) \Big] = 1 \iff \det[\boldsymbol{B}_1] = \det[\boldsymbol{B}_0]. \tag{47}$$

A straight forward computation then shows that (47) holds conditions (43) hold, as claimed. □

In particular, for the functions defined by relations (42), a simple computation reveals that $\kappa_{1,1} + \kappa_{1,2} = 0$ but

$$\kappa_{2,1} - \kappa_{2,2} = \sin(\tfrac{1}{2}(\vartheta_{n+1} - \vartheta_n)) \neq 0. \tag{48}$$

Therefore, in view of the result in the preceding lemma, we conclude that the mid-point rule formulated on the unreduced phase space P *cannot* be symplectic since the algorithmic flow in the reduced phase space $\widetilde{P}$ is not symplectic. This result may be extended to higher order 'symplectic' Runge-Kutta methods as the following sections will show.

Remarks. 3.2.

1. If expressions (48) are replaced by the conditions $\kappa_1 = \kappa_2 \equiv 1$, then algorithm (41) reduces to the conventional mid-point rule formulated *directly* on the reduced space $\tilde{P}$. When formulated directly on $\tilde{P}$, the midpoint rule retains its symplectic character since this reduced space is equipped with the canonical symplectic structure defined by (22).

2. Motivated by the structure of (41) we examine below this algorithm in its own right and, following Simo, Tarnow & Wong [1992], regard $\kappa_\alpha(\vartheta_n, \vartheta_{n+1})$ as arbitrary functions on $\widetilde{Q} \times \widetilde{Q}$ no longer defined by (48) and to be determined by enforcing energy conservation. □

3.3. Symplectic and E-M Algorithms on $\widetilde{P}$.

The preceding lemma does not rule out the construction, by a suitable choice of functions κ_α obeying restrictions (43), of a symplectic and energy-momentum conserving scheme within the class of algorithms (41). To explore this possibility, we compute the change in kinetic energy within a time-step predicted by this class of methods.

Multiplying $(41)_2$ by $\pi_{n+\frac{1}{2}}$ and using $(41)_1$ one obtains the algorithmic identity

$$\tilde{K}(\pi_{n+1}) - \tilde{K}(\pi_n) = -\frac{\kappa_2}{\kappa_1}\, g'_{n+\frac{1}{2}}\, \sin(\vartheta_{n+\frac{1}{2}})[\vartheta_{n+1} - \vartheta_n]. \tag{49}$$

Using elementary trigonometric identities, this expression can be rewritten as

$$\begin{aligned} \tilde{K}(\pi_{n+1}) - \tilde{K}(\pi_n) = \frac{\kappa_2}{\kappa_1}\, g'_{n+\frac{1}{2}}\, & \frac{(\vartheta_{n+1} - \vartheta_n)/2}{\sin(\frac{1}{2}(\vartheta_{n+1} - \vartheta_n))} \\ & \times\ [\cos(\vartheta_{n+1}) - \cos(\vartheta_n)]. \end{aligned} \tag{50}$$

Exact energy conservation requires

$$\tilde{K}(\pi_{n+1}) - \tilde{K}(\pi_n) = -[\tilde{V}(\vartheta_{n+1}) - \tilde{V}(\vartheta_n)], \tag{51}$$

where $\tilde{V}(\vartheta) := -g(\cos(\vartheta))$. Enforcement of this condition yields

$$\frac{\kappa_2}{\kappa_1} = \frac{\sin(\frac{1}{2}(\vartheta_{n+1} - \vartheta_n))}{\frac{1}{2}(\vartheta_{n+1} - \vartheta_n)} \left[\frac{g(\cos(\vartheta_{n+1})) - g(\cos(\vartheta_n))}{\cos(\vartheta_{n+1}) - \cos(\vartheta_n)}\right] \Big/ g'(\kappa_2 \cos(\vartheta_{n+\frac{1}{2}})). \tag{52}$$

Two gain insight into the nature of this result, consider the following situations:

i. Suppose that the function $g(\cdot)$ is at most linear. Then $g'(\cdot)$ is constant and the term within brackets in (52) is unity. By setting

$$\kappa_1 := \frac{(\vartheta_{n+1} - \vartheta_n)/2}{\sin(\frac{1}{2}(\vartheta_{n+1} - \vartheta_n))} \quad \text{and} \quad \kappa_2 = 1, \tag{53}$$

we obtain a symplectic and energy-momentum conserving algorithm since (53) satisfies conditions (43).

ii. If $g(\cdot)$ is arbitrary, it is not possible in general to simultaneously satisfy the energy condition (52) while obeying the symplectic restrictions (43). Furthermore, the solution of (52) for κ_2 is, at the very least, totally impractical. Nevertheless, an energy-momentum conserving algorithm is easily obtained by retaining expression $(53)_1$ for κ_1 and using (52) in $(41)_2$ to obtain

$$\left.\begin{aligned} \vartheta_{n+1} - \vartheta_n &= \Delta t \left[\frac{(\vartheta_{n+1} - \vartheta_n)/2}{\sin(\frac{1}{2}(\vartheta_{n+1} - \vartheta_n))}\right] \frac{\pi_{n+\frac{1}{2}}}{I_0} \\ \pi_{n+1} - \pi_n &= -\Delta t \left[\frac{g(\cos(\vartheta_{n+1})) - g(\cos(\vartheta_n))}{\cos(\vartheta_{n+1}) - \cos(\vartheta_n)}\right] \sin(\vartheta_{n+\frac{1}{2}}) \end{aligned}\right\}$$

This algorithm, however, is not symplectic.

In summary, the preceding analysis illustrates that, even in the *completely integrable* case, the construction of symplectic schemes that retain the property of energy conservation is not a trivial matter. The same conclusion holds for higher order accurate algorithms, such as the symplectic family of algebraically stable, implicit Runge-Kutta methods. These algorithms will not in general conserve energy, regardless of the accuracy order of the method, since the function $g(\cdot)$ is arbitrary.

3.4. Reconstruction: Conserving Schemes on P.

To illustrate the structure of a symplectic algorithm formulated directly on the unreduced phase space P, again within the simplest possible context, consider the dynamics of a spherical pendulum in a gravitational field and the one-parameter family of algorithms (41) with

$$\kappa_1 = \bar{\kappa}(\vartheta_{n+1} - \vartheta_n) \quad \text{and} \quad \kappa_2 \equiv 1. \tag{54}$$

Clearly, conditions (43) are satisfied so that these schemes are symplectic and contain the specific choice (53) as a particular case. The result below shows that the one-parameter family of algorithms on P given by

$$\left.\begin{aligned} \boldsymbol{q}_{n+1} - \boldsymbol{q}_n &= -\bar{\kappa}\,\Delta t\, \frac{\boldsymbol{q}_{n+\frac{1}{2}}}{\|\boldsymbol{q}_{n+\frac{1}{2}}\|} \times \frac{\boldsymbol{\pi}_{n+\frac{1}{2}}}{I_0}, \\ \boldsymbol{\pi}_{n+1} - \boldsymbol{\pi}_n &= - \Delta t\, \frac{\boldsymbol{q}_{n+\frac{1}{2}}}{\|\boldsymbol{q}_{n+\frac{1}{2}}\|} \times \nabla V\Big(\frac{\boldsymbol{q}_{n+\frac{1}{2}}}{\|\boldsymbol{q}_{n+\frac{1}{2}}\|}\Big). \end{aligned}\right\} \tag{55}$$

is obtained by *lifting* the reduced algorithmic dynamics (41) and (54) to the canonical phase space.

Lemma 3.3. Consider a force field with potential $V(\boldsymbol{q}) = -g(\boldsymbol{\gamma}\cdot\boldsymbol{q})$ and let $J_\gamma := \boldsymbol{\pi}\cdot\boldsymbol{\gamma}$ be the momentum map. The one-parameter family of symplectic algorithm on $\widetilde{P}$, defined by (41) and (54) is obtained via reduction of (55) defined on P to the level set $J_\gamma^{-1}(0)/S^1$, with

$$\bar{\kappa}(\vartheta) := \kappa_1(\vartheta)\,\mathrm{sin}[\tfrac{1}{2}\vartheta]/[\tfrac{1}{2}\vartheta] \quad \text{where} \quad \vartheta := \vartheta_{n+1} - \vartheta_n. \tag{56}$$

The symplectic-momentum preserving scheme in (53) corresponds to $\bar{\kappa} = 1$.

Proof. The proof that equations (55) reduce to (41) in the presence of a gravitational field employs the same calculation described in Section 3.2, with relation (39) now replaced by

$$\boldsymbol{\pi}_{n+\frac{1}{2}} = \frac{I_0}{\bar{\kappa}\Delta t}\,\frac{\boldsymbol{q}_n \times \boldsymbol{q}_{n+1}}{\|\boldsymbol{q}_{n+\frac{1}{2}}\|} = \frac{2\,I_0}{\Delta t\bar{\kappa}}\,\mathrm{sin}(\tfrac{1}{2}\vartheta)\,\boldsymbol{e}_2 \tag{57a}$$

and (40) replaced by

$$\vartheta_{n+1} - \vartheta_n = \Delta t\bar{\kappa}\Big[\frac{\frac{1}{2}\vartheta}{\mathrm{sin}(\frac{1}{2}\vartheta)}\Big]\pi_{n+\frac{1}{2}}/I_0. \tag{57b}$$

Equating (57) to $(41)_1$ one obtains (56). Similarly, equation $(55)_2$ reduces to $(41)_2$ with $\kappa_2(\vartheta) = 1$. □

Remarks. 3.3.

1. It can be shown that the preceding result with $\bar{\kappa} \equiv 1$ holds for the general case, i.e., the algorithm (55) is symplectic for an arbitrary potential $V(\boldsymbol{q})$. The following interpretation illustrates the difficulties involved in the formulation of symplectic algorithms when the phase space is a general manifold. Let

$$\bar{\boldsymbol{q}}_{n+\frac{1}{2}} := \frac{\boldsymbol{q}_{n+\frac{1}{2}}}{\|\boldsymbol{q}_{n+\frac{1}{2}}\|} \quad \text{and} \quad \mathbb{P}_{n+\frac{1}{2}} := \Big[\boldsymbol{I} - \bar{\boldsymbol{q}}_{n+\frac{1}{2}} \otimes \bar{\boldsymbol{q}}_{n+\frac{1}{2}}\Big], \tag{58}$$

and define $\bar{\boldsymbol{z}}_{n+\frac{1}{2}} \in P$ as the orthogonal projection of $\boldsymbol{z}_{n+\frac{1}{2}}$ onto P, i.e.,

$$\bar{\boldsymbol{z}}_{n+\frac{1}{2}} := (\bar{\boldsymbol{q}}_{n+\frac{1}{2}}, \bar{\boldsymbol{\pi}}_{n+\frac{1}{2}}) \quad \text{with} \quad \bar{\boldsymbol{\pi}}_{n+\frac{1}{2}} := \mathbb{P}_{n+\frac{1}{2}} \boldsymbol{\pi}_{n+\frac{1}{2}}. \tag{59}$$

The symplectic and momentum preserving algorithm (55) (with $\bar{\kappa} = 1$) can then be written as

$$\boldsymbol{z}_{n+1} - \boldsymbol{z}_n = \Delta t \mathbb{J}(\bar{\boldsymbol{q}}_{n+\frac{1}{2}}) \nabla H(\bar{\boldsymbol{z}}_{n+\frac{1}{2}}). \tag{60}$$

It follows that the mid-point rule, a one-stage implicit Runge-Kutta method, retains its symplectic character *if the intermediate stage* $\boldsymbol{z}_{n+\frac{1}{2}}$ *is projected onto* P via the orthogonal projection (58). The generalization of this result to general manifolds other than the unit sphere, although possible, leads to schemes with questionable practical effectiveness.

2. Energy conservation, on the other hand, can be easily enforced on the conventional midpoint rule approximation without upsetting conservation of the momentum map. For the problem at hand by defining $\bar{\kappa}(\boldsymbol{q}_n, \boldsymbol{q}_{n+1})$ via the difference quotient

$$\bar{\kappa}(\boldsymbol{q}_n, \boldsymbol{q}_{n+1}) := \frac{(\boldsymbol{q}_{n+1} - \boldsymbol{q}_n) \cdot \nabla V(\boldsymbol{q}_{n+\frac{1}{2}})}{V(\boldsymbol{q}_{n+1}) - V(\boldsymbol{q}_n)} \tag{61}$$

and omiting the scalings by $\|\boldsymbol{q}_{n+\frac{1}{2}}\|$ in (55) one arrives at an energy-momentum conserving algorithm which, however, is no longer symplectic. □

4. CONSERVING SCHEMES FOR STIFF ODE's.

The ultimate justification for any numerical method lies in improved performance. The objective of this section is to provide an assessment of the numerical performance of symplectic and energy-momentum algorithms. To demonstrate that the observed performance is generic, to be expected also for Hamiltonian systems on linear phase spaces, we consider a classical problem: the dynamics of N particles in $\mathbb{R}^3$ subjected to an interaction potential. For this problem conventional Gauss Runge-Kutta methods retain their symplectic character since the phase space is linear and the symplectic two-form is constant. The two objectives of this sections are (1) Demonstrate the inherit lack of stability of implicit symplectic schemes for stiff

problems, (2) Show that implicit energy-momentum methods are ideally suited for stiff systems.

First, we briefly summarize the form taken by Hamilton's equations. Next, we consider two representative examples of both symplectic and energy-momentum conserving algorithms. Although these two schemes are identical for linear Hamiltonian systems, the respective performance is dramatically different in the nonlinear regime. The chosen symplectic scheme, the conventional mid-point rule, is algebraically stable (see Hairer & Wanner [1991]) and unconditionally A-stable in the linear regime and, nevertheless, exhibits blow-up in finite time in the nonlinear regime. The reason for this lack of stability is to be found in the lack of dissipation of symplectic schemes and the presence of a double root for infinite sample frequencies. As a result, high frequencies not resolved in the time discretization are 'seen' by the algorithm as infinite sample frequencies leading inevitably to weak (polynomial) instability. In sharp contrast with this result, we show that the energy-momentum conserving scheme remains stable.

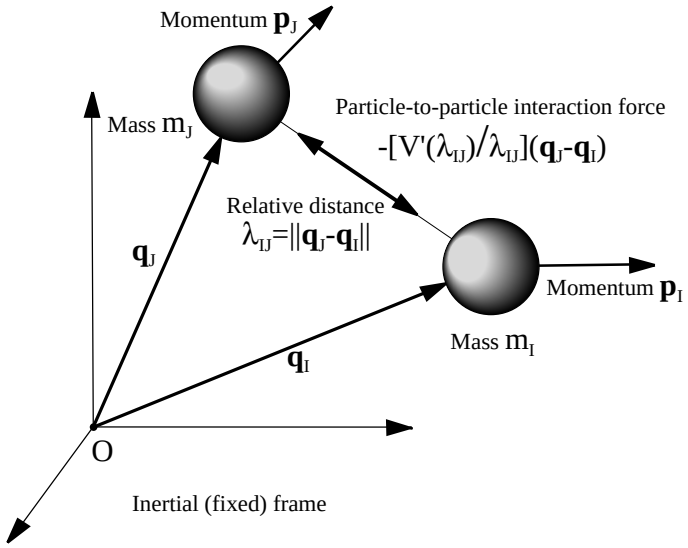

FIGURE 2. The motion of N-particles in the ordinary Euclidean space subject to a particle-to-particle interaction potential.

4.1. The N-Particle Problem: Hamiltonian Structure.

Consider N particles each with mass $m_I > 0$, position vector $\boldsymbol{q}_I$ and momentum $\boldsymbol{p}_I = m_I\,\boldsymbol{q}_I$, $(I = 1, 2, \cdots, N)$. The configuration and phase spaces are, therefore,

$$Q \approx \mathbb{R}^{3N} \quad \text{and} \quad P = T^*Q \approx \mathbb{R}^{3N} \times \mathbb{R}^{3N}. \tag{62}$$

We shall denote by $\boldsymbol{z} = (\mathbf{q}, \mathbf{p}) \in P$ an arbitrary point in the phase space, and use the notation

$$\mathbf{q} = (\boldsymbol{q}_1, \cdots, \boldsymbol{q}_N) \in Q \quad \text{and} \quad \mathbf{p} = (\boldsymbol{p}_1, \cdots, \boldsymbol{p}_N) \in \mathbb{R}^{3N}. \tag{63}$$

The system so defined is subjected to an interaction potential depending only on the relative distances between particles. A typical example is furnished by Newton's inverse square law. The Hamiltonian $H: P \to \mathbb{R}$ for the system at hand is separable, of the form $H(\boldsymbol{z}) = K(\mathbf{p}) + V(\mathbf{q})$, with

$$K(\mathbf{p}) := \sum_{I=1}^{N} \tfrac{1}{2} m_I^{-1} \, \|\boldsymbol{p}_I\|^2, \quad V(\mathbf{q}) := \sum_{I=1}^{N-1} \sum_{J=I+1}^{N} \widetilde{V}(\lambda_{IJ}), \tag{64}$$

where $\lambda_{IJ} = \lambda_{JI} := \|\boldsymbol{q}_J - \boldsymbol{q}_I\|$ is the relative distance between particle m_I and particle m_J. Observe that the potential function $\widetilde{V} : \mathbb{R} \to \mathbb{R}$ is completely arbitrary. The phase space P is equipped with the (constant) canonical symplectic two-form

$$\Omega(\delta \boldsymbol{z}_1, \delta \boldsymbol{z}_2) = \delta \boldsymbol{z}_1 \cdot \mathbb{J} \delta \boldsymbol{z}_2 \quad \text{where} \quad \mathbb{J} := \begin{bmatrix} \mathbf{0} & \mathbf{1} \\ -\mathbf{1} & \mathbf{0} \end{bmatrix}. \tag{65}$$

The motion of the system is governed by Hamilton's canonical equations given by

$$\dot{\boldsymbol{z}} = \mathbb{J} \nabla H(\boldsymbol{z}) \iff \begin{cases} \dot{\boldsymbol{q}}_I = \boldsymbol{p}_I / m_I \\ \dot{\boldsymbol{p}}_I = \sum\limits_{\substack{J=1 \\ J \neq I}}^{N} \sigma_{IJ} \, (\boldsymbol{q}_J - \boldsymbol{q}_I) \end{cases} \tag{66}$$

where for our subsequent developments we have defined the $N(N+1)/2$ coefficients σ_{IJ} as

$$\sigma_{IJ} = \widetilde{V}'(\lambda_{IJ}) / \lambda_{IJ} = \sigma_{JI}. \tag{67}$$

In addition to the usual preservation of the symplectic two-form by the Hamiltonian flow, the system possesses the following conserved quantities.

i. *Conservation of energy.* Since the Hamiltonian is autonomous it follows that H is conserved by the dynamics.

ii. *Conservation of momentum.* The Hamiltonian is obviously invariant under translations and rotations, i.e., under the (symplectic) action of the Euclidean group on P. It follows that the momentum maps

$$\boldsymbol{L}(\boldsymbol{z}) := \sum_{I=1}^{N} \boldsymbol{p}_I \quad \text{and} \quad \boldsymbol{J}(\boldsymbol{z}) := \sum_{I=1}^{N} \boldsymbol{q}_I \times \boldsymbol{p}_I \tag{68}$$

are conserved quantities by the dynamics. These are the familiar laws of conservation of the total linear momentum and the total angular momentum of the system.

4.2. Symplectic, Momentum Conserving Algorithm.

Let $\boldsymbol{z}_n \in P$ be prescribed initial data at time t_n and consider the following family of algorithms for the approximation of (66) in the interval $[t_n, t_{n+1}]$

$$\left.\begin{aligned} \boldsymbol{q}_I^{n+1} - \boldsymbol{q}_I^n &= \Delta t\, \boldsymbol{p}_I^{n+(1-\alpha)}/m_I \\ \boldsymbol{p}_I^{n+1} - \boldsymbol{p}_I^n &= \Delta t \sum_{\substack{J=1 \\ J\neq I}}^{N} \sigma_{IJ}\,(\boldsymbol{q}_J^{n+\alpha} - \boldsymbol{q}_I^{n+\alpha}) \end{aligned}\right\} \tag{69}$$

where

$$\left.\begin{aligned} \boldsymbol{q}_I^{n+\alpha} &:= \alpha \boldsymbol{q}_I^{n+1} + (1-\alpha)\boldsymbol{q}_I^n, \\ \boldsymbol{p}_I^{n+(1-\alpha)} &:= (1-\alpha)\boldsymbol{p}_I^{n+1} + \alpha \boldsymbol{p}_I^n. \end{aligned}\right\} \tag{70}$$

and $\alpha \in [0,1]$ is an algorithmic parameter. Regarding σ_{IJ} as $N(N+1)/2$ algorithmic parameters, it follows that the approximation (69) depends on $N(N+1)/2+1$ parameters which remain to be specified in order to achieve desired conservation properties while maintaining consistency. Before doing so, we make the following observation.

Lemma 4.1. The algorithmic approximation (69) preserves exactly the momentum maps defined by (68) for any $\alpha \in [0,1]$ and arbitrary σ_{IJ}, provided that the *symmetry* condition $\sigma_{IJ} = \sigma_{JI}$ holds.

Proof. The claim follows from a direct computation. Conservation of angular momentum follows from the identity

$$\begin{aligned} \boldsymbol{J}(\boldsymbol{z}_{n+1}) - \boldsymbol{J}(\boldsymbol{z}_n) = \sum_{I=1}^{N} \Big[& \boldsymbol{q}_I^{n+\alpha} \times (\boldsymbol{p}_I^{n+1} - \boldsymbol{p}_I^n) \\ & + (\boldsymbol{q}_I^{n+1} - \boldsymbol{q}_I^n) \times \boldsymbol{p}_I^{n+(1-\alpha)} \Big], \end{aligned} \tag{71}$$

along with the algorithmic equations (69), the symmetry condition $\sigma_{IJ} = \sigma_{JI}$ and the skew-symmetry property $\boldsymbol{q}_I^{n+\alpha} \times \boldsymbol{q}_J^{n+\alpha} = -\boldsymbol{q}_J^{n+\alpha} \times \boldsymbol{q}_I^{n+\alpha}$. Conservation of linear momentum is obvious. □

Remarks. 4.1.

1. Consider the one-parameter family of algorithms obtained by setting

$$\sigma_{IJ} = \frac{\widetilde{V}'(\lambda_{IJ}^{n+\alpha})}{\lambda_{IJ}^{n+\alpha}} \quad \text{with} \quad \lambda_{IJ}^{n+\alpha} := \|\boldsymbol{q}_J^{n+\alpha} - \boldsymbol{q}_I^{n+\alpha}\|. \tag{72}$$

It can be easily shown that these algorithms are symplectic for any $\alpha \in [0,1]$, while conditionally A-stable and only first order accurate if $\alpha \neq \frac{1}{2}$; see Simo, Tarnow & Wong [1992].

2. For $\alpha \equiv \frac{1}{2}$ algorithm (69) together with (72) reduces to the conventional mid-point rule; a scheme well-known to be algebraically stable (and hence B-stable). By the preceding lemma, the scheme is also exact momentum preserving. This is the symplectic algorithm used in the simulations reported below. □

4.3. Energy and Momentum Conserving Algorithm.

Next we construct an exact energy and momentum preserving algorithm via suitable definition of the algorithmic parameters σ_{IJ} in the family of algorithms (69). For simplicity, we shall restrict the subsequent discussion to the case $\alpha = \frac{1}{2}$.

To compute the change in energy within a time step $[t_n, t_{n+1}]$, we observe that the change in kinetic energy can be written in view of (64) as

$$K(\mathbf{p}^{n+1}) - K(\mathbf{p}^n) = \sum_{I=1}^{N} m_I^{-1} \, (\boldsymbol{p}_I^{n+1} - \boldsymbol{p}_I^n) \cdot \boldsymbol{p}_I^{n+\frac{1}{2}}. \tag{73}$$

Substituting equations (69) into the above identity yields, after straight forward manipulations, the result

$$K(\mathbf{p}^{n+1}) - K(\mathbf{p}^n) = -\sum_{I=1}^{N-1} \sum_{J=I+1}^{N} \tfrac{1}{2}\sigma_{IJ}(\lambda_{IJ}^{n+1} - \lambda_{IJ}^n)(\lambda_{IJ}^{n+1} + \lambda_{IJ}^n) \tag{74}$$

Conservation of energy conservation requires $K(\mathbf{p}^{n+1}) - K(\mathbf{p}^n) = -[V(\mathbf{q}^{n+1}) - V(\mathbf{q}^n)]$. In view of $(64)_2$, by setting

$$\boxed{\sigma_{IJ} = \frac{1}{\frac{1}{2}(\lambda_{IJ}^{n+1} + \lambda_{IJ}^n)} \, \frac{\widetilde{V}(\lambda_{IJ}^{n+1}) - \widetilde{V}(\lambda_{IJ}^n)}{\lambda_{IJ}^{n+1} - \lambda_{IJ}^n},} \tag{75}$$

this condition is automatically enforced and exact energy conservation holds.

Remarks. 4.2.

1. Use of expression (75) as a definition for σ_{IJ} amounts to replacing the derivative $\widetilde{V}'(\lambda_{IJ}^{n+\frac{1}{2}})$ in (72) by a difference quotient and the distance $\lambda_{IJ}^{n+\frac{1}{2}}$ by the average of the distances $\frac{1}{2}(\lambda_{IJ}^{n+1} + \lambda_{IJ}^n)$. For the one-dimensional problem, the idea of replacing the derivative of the potential by a finite difference quotient goes back to Labudde & Greenspan [1976].

2. Algorithm (69) together with (75) and $\alpha = \frac{1}{2}$ is the exact energy-momentum scheme tested in the simulations described below. □

4.4. Numerical Results.

Here we present numerical examples for the symplectic mid-point rule given by (69) and (72) with $\alpha = \frac{1}{2}$ and the energy-momentum conserving algorithm given by (69) and (75). We take the case of four particles ($N = 4$) and use a nonlinear spring interaction potential

$$\widetilde{V}(\lambda_{IJ}) = \frac{1}{2} k_{IJ}(\lambda_{IJ} - L_{IJ})^2, \tag{76}$$

where k_{IJ} is the modulus of the spring joining particle I to particle J and L_{IJ} is the natural length.

Figure 3 summarizes the simulation results obtained for the four-particle problem, mases $m_1 = m_2 = m_3 = m_4 = 1$, and the following initial conditions:

$$\begin{aligned}
\mathbf{q}_1 &= (0,0,0)^{\mathrm{T}} & \mathbf{p}_1 &= (0,0,0)^{\mathrm{T}} \\
\mathbf{q}_2 &= (0.8983, 0.5616, 0)^{\mathrm{T}} & \mathbf{p}_2 &= (-0.0500, 0.0866, 0)^{\mathrm{T}} \\
\mathbf{q}_3 &= (0, 1.0010, 0)^{\mathrm{T}} & \mathbf{p}_3 &= (0, -0.1000, 0)^{\mathrm{T}} \\
\mathbf{q}_4 &= (0.2589, 0.5987, 0.7580)^{\mathrm{T}} & \mathbf{p}_4 &= (-0.0500, 0.0288, 0)^{\mathrm{T}}
\end{aligned}$$

$$\begin{aligned}
k_{12} &= \text{1E02} & L_{12} &= 1 \\
k_{13} &= \text{1E04} & L_{13} &= 1 \\
k_{14} &= \text{1E06} & L_{14} &= 1 \\
k_{23} &= \text{1E07} & L_{23} &= 1 \\
k_{24} &= \text{5E03} & L_{24} &= 1 \\
k_{34} &= \text{5E02} & L_{34} &= 1
\end{aligned}$$

Shown in the figure are the total energy and total angular momentum of the system which were calculated from *converged* solutions to the algorithmic equations for three time steps: $\Delta t = .04, .03$, and $.02$. These time steps were chosen on the basis of linearized frequencies at the reference (unstressed) configuration. Linearization of the potential at the reference configuration yields a stiffness matrix with a frequency range (excluding rigid body modes) of $\omega_{min} \approx 12$ and $\omega_{max} \approx 4470\ rad/sec$. The above time steps correspond to approximately 12, 16, and 25 sample points on the low mode, respectively. The configuration given in the initial condition was such that nearly all of the potential energy was contained in the softest springs. This was done as an attempt to not artificially excite the 'high modes' in the system.

As shown in Figure 3, the midpoint rule does not conserve the total energy of the system. In particular, for time steps of $\Delta t = .04$ and $.03$ the energy grows exponentially. For the time step $\Delta t = .02$ the total energy oscillates about its initial value and the amplitude remains bounded after more than 5×10^5 steps. The total angular momentum, on the other hand, is conserved for all three time steps. (This is due to the fact that the results are for converged solutions to the algorithmic equations.) In contrast to the results for the midpoint rule, the energy-momentum method exactly conserves both total energy and angular momentum for all three time step sizes.

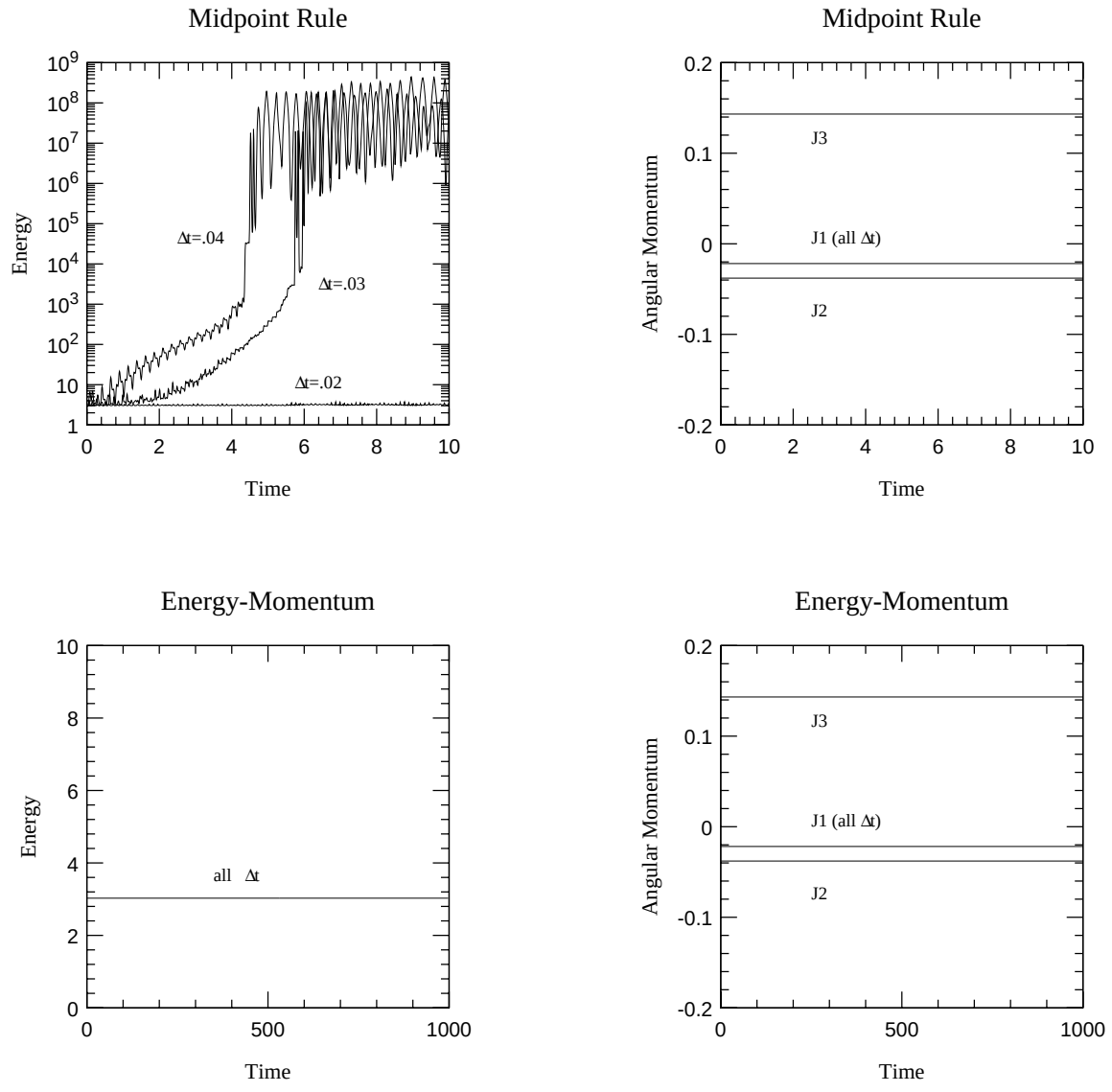

FIGURE 3. Simulation results for the four-particle problem. The plots show total energy and angular momentum calculated from converged solutions to the algorithmic equations.

5. CONCLUDING REMARKS.

In the preceding analysis we have shown that the mid-point rule, the classical symplectic Runge-Kutta method, fails to retain its symplectic character for general Hamiltonian systems when the symplectic two-form is non-constant. For instance, we have shown that in order to render the mid-point rule symplectic, a projection of the intermediate stage onto the phase space is required. This is a manifestation of a

general fact. For Hamiltonian systems with constraints, but with an underlying linear phase space, it is possible to modify the conventional algorithms as to retain their the symplectic character by introducing Lagrange multipliers. A general methodology for this construction is described in Jay [1993]. This construction, however, fails if the symplectic two-form is non-constant.

Even if the construction of symplectic schemes is practically feasible, this class of algorithms is not suitable for the solution of stiff problems. In this situation, implicit methods are used as a means of retaining unconditional stability without resolving the high frequency present in the problem. By construction, symplectic method cannot have any numerical dissipation since complex roots of the amplification matrix must lie on the unit circle and, moreover, exhibits multiple roots at infinite sampling frequencies. The mid-point rule provides a representative example that illustrates these features. As a result, the unresolved high–frequencies in the problem are seen by a symplectic algorithm as infinite sampling frequencies, thus triggering a weak instability phenomenon that leads to an eventual blow-up of the scheme. These result have been verified numerically in numerical simulations. In sharp contrast with symplectic methods, we have shown that energy-momentum algorithms provide the required control on the unresolved high-frequencies without resorting to numerical dissipation, thus leading to unconditionally stable schemes. These methods are therefore ideally suitable for the long–term numerical simulation of a stiff systems such as those arising in rigid–body dynamics. We remark that fouth order accurate methods can be constructed from second order accurate methods as composite algorithms which retain stability and conservation properties, see Tarnow & Simo [1992] for additional details.

Acknowledgements. This research was supported by AFOSR under Contract No. 2-DJA-826 with Stanford University. This support is gratefully acknowledged.

6. REFERENCES.

R. Abraham & J.E. Marsden [1978] *Foundations of Mechanics,* Second Edition, Addison-Wesley.

M. Austin, P.S. Krishnaprasad & L.C. Chen [1992] "Almost Lie-Poisson Integrators for Rigid Body Dynamics," *J. Computational Physics,* in press.

A. Bayliss & E. Isaacson [1975] "How to Make Your Algorithm Conservative," *American Mathematical Society*, A594–A595.

P.J. Chanell & C. Scovel [1990] "Symplectic Integration of Hamiltonian Systems," *Nonlinearity,* **3**, 231–259.

Feng Kang [1986] "Difference Schemes for Hamiltonian Formalism and Symplectic Geometry," *J. Computational Mathematics,* **4**, 279–289.

L. Jay, [1993], "Symplectic Partitioned Runge–Kutta Methods for Constrained Hamiltonian Systems," *University de Genéve*, Preprint.

G. Zhong & J.E. Marsden [1988] "Lie-Poisson Hamilton-Jacobi Theory and Lie-Poisson Integrators," *Physics Letters A,* **3**, 134–139.

E. Hairer & G. Wanner [1991] *Solving Ordinary Differential Equations II,* Springer Verlag, Berlin.

R.A. LaBudde & D. Greenspan [1976a] "Energy and Momentum Conserving Methods of Arbitrary Order for the Numerical Integration of Equations of Motion. Part I," *Numerisch Mathematik*, **25**, 323–346.

R.A. LaBudde & D. Greenspan [1976b] "Energy and Momentum Conserving Methods of Arbitrary Order for the Numerical Integration of Equations of Motion. Part II," *Numerisch Mathematik*, **26**, 1–16.

F.M. Lasagni [1988] "Canonical Runge–Kutta Methods," *ZAMP,* **39**, 952-953.

J.M. Sanz-Serna [1988] "Runge–Kutta Schemes for hamiltonian Systems," *BIT,* **28**, 877–883.

J.M. Sanz-Serna [1992] "Symplectic Integration for Hamiltonian Problems: An Overview," *Acta Numerica,* **1**, 143-386.

C. Scovel [1991] "Symplectic Numerical Integration of Hamiltonian Systems," in *The Geometry of Hamiltonian Systems*, Proceedings of the Workshop held June 5th to 15th, 1989, pp. 463–496, Tudor Ratiu Editor, Springer-Verlag.

J.C. Simo & K.K. Wong [1991] "Unconditionally Stable Algorithms for Rigid Body Dynamics that Exactly Preserve Energy and Angular Momentum," *International J. Numerical Methods in Engineering,* **31**, 19–52.

J.C. Simo, N. Tarnow & K. Wong [1992] "Exact Energy Momentum Conserving Algorithms and Symplectic Schemes for Nonlinear Dynamics," *Computer Methods in Applied Mechanics and Engineering,* **1**, 63–116.

J.C. Simo & N. Tarnow [1992a] "The Discrete Energy Momentum Method. Conserving Algorithms for Nonlinear Elastodynamics," *ZAMP,* **43**, 757–793.

J.C. Simo & N. Tarnow [1992b] "A New Energy Momentum Method for the Dynamics of Nonlinear Shells," *International J. Numerical Methods in Engineering*, in press.

J.C. Simo, N. Tarnow & M. Doblaré [1992c], "Exact Energy–Momentum Algorithms for the Dynammics of Nonlinear Rods," *International J. Numerical Methods in Engineering*, in press.

N. Tarnow & J.C. Simo, [1992] "How to Render Second Order Accurate Time–Stepping Algorithms Fourth Order Accurate While Retaining Their Stability and Conservation Properties" *Computer Methods in Applied Mechanics and Engineering,* in press.

R. de Vogelaere [1956] "Methods of Integration which Preserve the Contact Transformation Property of Hamiltonian Equations," *Department of Mathematics, University of Notre Dame,* Report **4**.